

Analysis of the lowest $4f \rightarrow 5d$ two-photon transition in $Ce^{3+}:CaF_2$

S. K. Gayen,* D. S. Hamilton, and R. H. Bartram

Department of Physics and Institute of Materials Science, University of Connecticut, Storrs, Connecticut 06268

(Received 14 August 1986)

A theoretical estimate of the two-photon absorption (TPA) cross section for the lowest $4f \rightarrow 5d$ zero-phonon transition in $Ce^{3+}:CaF_2$ is presented. A point-charge crystal-field model is used to calculate the odd component of the C_{4v} crystal field which mixes states of opposite parity into the initial and final states participating in the transition. The sum over intermediate states is evaluated by assuming a constant energy denominator and using a closure approximation. The calculated magnitude and polarization anisotropy of the TPA cross section are compared with the experimentally measured values and methods to improve the calculation are discussed.

I. INTRODUCTION

In their pioneering experiment in 1961, Kaiser and Garret¹ first experimentally demonstrated two-photon absorption (TPA) in the rare-earth-ion-doped crystal $Eu^{2+}:CaF_2$. However, most of the subsequent experimental and theoretical investigations of TPA in rare-earth-ion-doped solids have studied the sharp, parity-allowed $4f \rightarrow 4f$ non-phonon transitions. In this paper we will present a calculation of the TPA cross section and its polarization anisotropy for the first-order parity-forbidden $4f \rightarrow 5d$ non-phonon transition in $Ce^{3+}:CaF_2$. Although the previously developed theories for the $4f \rightarrow 4f$ two-photon transitions will not be applicable here, we will compare to much of that work in this calculation and hence provide a short review in Sec. II. Then the characteristics of $Ce^{3+}:CaF_2$ relevant to our calculation are presented, along with a summary of the experimental TPA measurements in this crystal. The essential role of the crystal field in mixing the $4f$ and $5d$ wave functions will be considered next. It is this mixing which lifts the parity selection rule for the transition. The odd component of the crystal field, which is responsible for this mixing, is developed using a point-charge model involving a charge-compensating F^- ion which is located nearby the cerium ion. The first-order perturbation correction to the $Ce^{3+}:CaF_2$ wave functions is then calculated. These parity-mixed initial- and final-state wave functions are then used to obtain a theoretical estimate of the TPA cross section and its polarization anisotropy for the zero-phonon transition. The sum over the intermediate states which appears in the calculation is evaluated by assuming a constant energy denominator for all of the intermediate states and then using a closure approximation. The calculated polarization anisotropy of the TPA cross section as well as its magnitude is then compared to the experimental values.

II. THEORETICAL REVIEW

For the general case of impurity ions in solids, the TPA cross section per photon per ion in the electric-dipole approximation is given by²⁻⁴

$$\sigma = \frac{4\pi^2 e^4}{\hbar^2 c^3} (\eta_1 \eta_2)^2 \frac{\nu_1 \nu_2}{n_1 n_2} L(\nu) \times \left| \sum_i \left[\frac{\langle f | \hat{e}_1 \cdot \mathbf{r} | i \rangle \langle i | \hat{e}_2 \cdot \mathbf{r} | g \rangle}{\nu_{ig} - \nu_2} + \frac{\langle f | \hat{e}_2 \cdot \mathbf{r} | i \rangle \langle i | \hat{e}_1 \cdot \mathbf{r} | g \rangle}{\nu_{ig} - \nu_1} \right] \right|^2, \quad (1)$$

where $|g\rangle$, $|i\rangle$, and $|f\rangle$ are the ground, intermediate, and final states of the transition, $L(\nu)$ is the normalized line-shape function, and ν_{ig} is the ground to intermediate state splitting in cm^{-1} . The subscripts 1 and 2 denote the particular photon with a frequency in cm^{-1} and a polarization unit vector of \hat{e} . The index of refraction at that frequency is n and the local-field correction is η .

Even for a moderately complex atom it is difficult to enumerate all of the intermediate states, and impractical to carry out the sum over them directly. Axe has developed an approximate method⁵ to evaluate the sum for the $4f \rightarrow 4f$ TPA transitions for the rare-earth (\mathcal{R}) ions. An expression similar to that appearing within the large parentheses in Eq. (1) also appears in the Judd-Ofelt theory^{6,7} of one-photon electric-dipole absorption between mixed-parity states of \mathcal{R}^{3+} ions in crystals, where the role of the second photon is taken by the odd-parity component of the crystal field. Judd and Ofelt showed that the sum over intermediate states could be evaluated by using a closure approximation in which the energy denominator is assumed constant for each excited configuration. Axe used a closure approximation in a second-order theory which successfully predicted the line strengths of a number of intra- $4f$ TPA transitions for several rare-earth ions. However, recent TPA measurements^{8,9} in $Gd^{3+}:LaF_3$ indicated the inadequacy of this theory. Compared to the predictions of Axe's second-order theory, most of the observed TPA transitions were anomalously strong, were highly dependent on the direction of the polarization with respect to the crystal axes of the host, and violated the angular momentum selection rule of $\Delta J \leq 2$. Some of the observed transitions violated

the $\Delta S=0$ and $\Delta L \leq 2$ selection rules as well. These observations, in turn, led to new theoretical endeavors. Judd and Pooler¹⁰ expanded the second-order theory to include third-order terms involving the spin-orbit interaction within the levels of the intermediate configurations and showed that the $\Delta S=0$ selection rule is lifted in third order. Downer and Bivas¹¹ have shown that the inclusion of the crystal-field interaction among the intermediate states can relax both the $\Delta L \leq 2$ and $\Delta J \leq 2$ selection rules in third order. They invoked fourth-order corrections involving the spin-orbit and crystal-field interactions and found that these higher-order corrections may be comparable with and even stronger than the second-order contribution. The theory thus developed has been successfully used to obtain quantitative agreement between calculated and measured values for the TPA line strengths and polarization anisotropy of the $4f^7 \rightarrow 4f^7$ transitions of Eu^{2+} in CaF_2 and SrF_2 crystals¹² and of the $^3H_4 \rightarrow ^1S_0$ transition¹³ in $\text{Pr}^{3+}:\text{LaF}_3$. More recently, Reid and Richardson¹⁴ have pointed out that ligand-dependent effects are also important in the higher-order TPA intensity analysis. They demonstrated that the dynamic ligand polarization terms in third-order perturbation can make a contribution comparable to those associated with the static crystal-field perturbations.

Thus one now has a well-developed theory for the $4f$ intraconfigurational two-photon transitions in rare-earth-ion-doped insulators. However, the theory mentioned above is not applicable to the first-order parity-forbidden $4f \rightarrow 5d$ transitions which we have observed in $\text{Ce}^{3+}:\text{CaF}_2$.¹⁵⁻¹⁷ In this paper we begin the development of a theory for the purely electronic two-photon $4f \rightarrow 5d$ transition in $\text{Ce}^{3+}:\text{CaF}_2$.

III. EXPERIMENTAL REVIEW

In this section we present a brief review of the experimental results and the characteristics of $\text{Ce}^{3+}:\text{CaF}_2$ to make the present discussion self-contained. Details of the experimental apparatus and techniques have been described elsewhere.¹⁵⁻¹⁷

In low-concentration and oxygen-free samples, the dominant site symmetry of the trivalent cerium ion is C_{4v} .¹⁸ The Ce^{3+} ion substitutes for a Ca^{2+} ion and is charge compensated by an F^- ion in the next-body centered interstitial site. The interaction between the charge-compensating F^- ion and the single optically active electron of the Ce^{3+} ion induces a tetragonal distortion which lowers the Ce^{3+} site symmetry from O_h to C_{4v} . The crystal-field and spin-orbit interactions completely remove the orbital degeneracy of the $4f$ and the $5d$ states leaving only the Kramer's degeneracy. The $4f$ orbital splits into the $^2F_{5/2}$ and $^2F_{7/2}$ manifolds separated by about 2000 cm^{-1} .

Two identical photons from a frequency-tunable dye laser were used to induce the $4f \rightarrow 5d$ transitions for the measurements in $\text{Ce}^{3+}:\text{CaF}_2$. The two-photon excitation spectrum displayed in Fig. 1 is from the lowest Stark component of the $^2F_{5/2}$ manifold to the lowest of the $5d$ states. The sharp zero-phonon line at the low-energy end of the spectrum is the purely electronic transition between

the two states. The appearance of the zero-phonon line in the TPA spectrum of this first-order parity-forbidden two-photon transition may be explained in terms of the crystal-field parity mixing among the participating states. Since the Ce^{3+} ion is at a site which lacks a center of inversion, the crystal field can mix the $5d$ states with the $4f$ ground state and the $4f$ states with the lowest $5d$ state. The parity selection rule is thus relaxed, and a two-photon transition between mixed-parity states becomes possible. The measured peak value¹⁵ of the TPA cross section for the zero-phonon transition is of the order $10^{-54} \text{ cm}^4 \text{ sec}$, which indicates that the odd-parity component of the C_{4v} crystal field in $\text{Ce}^{3+}:\text{CaF}_2$ is very effective in mixing the required states of opposite parity.

A special feature of the lowest $4f \rightarrow 5d$ TPA transition in $\text{Ce}^{3+}:\text{CaF}_2$ is that both the zero-phonon line and its phonon sideband have comparable strength. The origin of the phonon sideband here is rather complex. The zero-phonon line and the vibrational progressions built on it appear in the TPA spectrum because of the parity mixing of the odd crystal-field components. However, vibronic coupling also induces phonon-assisted transitions of comparable intensity, so that totally symmetric progressions built on false origins are also observed. The overall spectrum is a superposition of all of the contributions. The lowest $4f \rightarrow 5d$ two-photon transition in $\text{Ce}^{3+}:\text{CaF}_2$ thus combines the features of an allowed two-photon transition with those of a parity-forbidden but vibronically induced two-photon transition.

The TPA cross section for the zero-phonon transition shows a strong dependence on the polarization direction of the incident laser beam as noted in Fig. 2. Measurements of the polarization anisotropy of the TPA cross section for the zero-phonon transition and its analysis¹⁵ following the general group-theoretical formalism^{19,20} confirm the C_{4v} symmetry of the cerium site, and reveal that for the case of two identical photons, only A_1 and E

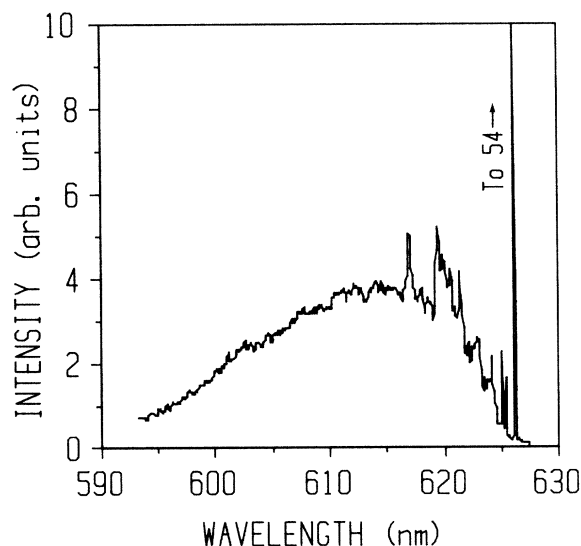


FIG. 1. Composite two-photon excitation spectrum of 0.003 at. % $\text{Ce}^{3+}:\text{CaF}_2$ at a 6-K sample temperature. The fluorescence intensity has been point-by-point normalized to the square of the dye-laser power. The dye-laser beam is along the $[100]$ axis and is linearly polarized 45° to the $[010]$ axis.

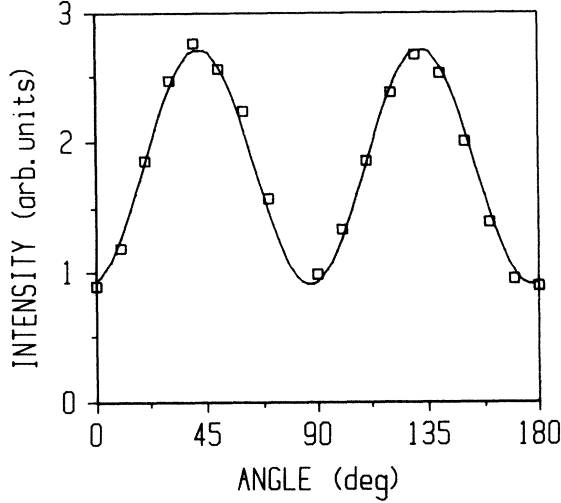


FIG. 2. Polarization dependence of the two-photon absorption cross section for the zero-phonon transition at a 6-K sample temperature. The dye-laser beam is incident along the [100] axis and the angle θ is measured from the [010] axis of the host crystal. The squares represent the experimental measurements and the curve is a fit to the data using the angular function of Eq. (2).

symmetry transitions contribute to the total TPA transition probability. For a laser beam incident along the [100] axis of the CaF_2 host, the TPA cross section as a function of the polarization direction is given by the relation¹⁵

$$\sigma(\theta) = a + b \sin^2(2\theta), \quad (2)$$

where θ is the angle between the polarization vector and the [010] axis, and a and b are functions of both the photon frequency and the matrix elements between the states participating in the transition. The polarization anisotropy,

$$A = \frac{\sigma(45^\circ) - \sigma(0^\circ)}{\sigma(45^\circ) + \sigma(0^\circ)}, \quad (3)$$

is 0.50 for the zero-phonon transition.

The polarization dependence of the TPA cross section for the phonon sideband is more complex than for the zero-phonon line. At large frequency shifts from the zero-phonon line, the cross section was found to be independent of laser polarization, while at smaller shifts of less than 500 cm^{-1} , the polarization anisotropy is frequency dependent. This behavior of the polarization anisotropy may be qualitatively understood by noting that for small frequency shifts, the TPA spectrum is dominated by the a_1 -phonon sideband of the zero-phonon transition, which shares its polarization anisotropy, whereas for the larger shifts, false origins and their associated a_1 -phonon sidebands make a comparable contribution to the spectrum. Since the polarization anisotropy of the false origins is different from that of the zero-phonon line, the combined spectrum tends to be isotropic in this region.

IV. CRYSTAL-FIELD MIXING OF WAVE FUNCTIONS

The major contribution to the odd-parity components of the C_{4v} crystal field comes from the interaction between the single optically active electron of the Ce^{3+} ion and the F^- charge compensator. We use a point-charge crystal-field model for the F^- charge compensator. The potential energy due to such a point charge situated at \mathbf{r}_0 in the field of the single optically active Ce^{3+} electron at \mathbf{r} is

$$V = -e^2/\epsilon |\mathbf{r} - \mathbf{r}_0|, \quad (4)$$

where ϵ is an effective dielectric constant. We now choose our coordinate system such that its origin is at the nucleus of the Ce^{3+} ion and the [100], [010], and [001] axes are the x , y , and z coordinate axes, respectively. We also assume that the charge compensator is at the nearest interstitial site along the [001] axis. Then \mathbf{r}_0 will be along the z direction with magnitude $a/2$, where a is the lattice constant of CaF_2 . Denoting the position of the Ce^{3+} $4f$ electron by $\mathbf{r} = (r, \theta, \phi)$ we can write V as

$$V = -(e^2/\epsilon r_0) \sum_{l=0}^{\infty} (r/r_0)^l P_l(\cos\theta), \quad (5)$$

where $r < r_0$ and we have used the addition theorem for the spherical harmonics. The odd component of the crystal field corresponds to odd values of l in the expansion. Since $r/r_0 \ll 1$, the higher-order terms become successively smaller, and to a first approximation we keep only the lowest order ($l=1$) term. Thus the potential due to the odd component of the crystal field can be expressed as

$$V_{\text{odd}} = - \left[\frac{4\pi}{3} \right]^{1/2} \frac{e^2}{\epsilon r_0^2} r Y_1^0(\theta) = - \frac{e^2}{\epsilon r_0^2} z. \quad (6)$$

The distortion of the cubic CaF_2 lattice due to the presence of the charge compensator and the interaction of the charge compensator with other ligands have been neglected in arriving at Eq. (6). The contributions of these effects are not negligible but will not change the overall symmetry. Accordingly, they may be incorporated phenomenologically in ϵ . We may also include in ϵ the effects of shielding by the ligands and by the filled $5s$ and $5p$ orbitals of the Ce^{3+} ion.²¹ Consequently, the value of ϵ is quite uncertain. Nevertheless, it should be noted that, in the present work, the *form* of the odd-parity component of the crystal field is known *a priori*, in contrast with the assumptions in the Judd-Ofelt treatment of the $4f \rightarrow 4f$ one-photon transitions.^{6,7}

We now consider the basis functions to be used in this calculation. We are concerned with the purely electronic two-photon transition from the lowest $4f$ ground state to the lowest $5d$ excited state and need to calculate the admixtures of other states with these two states due to the perturbation V_{odd} . For the basis functions belonging to these two states, we take the wave functions which correspond to the crystal-field and spin-orbit-coupling split lowest $4f$ and lowest $5d$ levels, respectively. Manthey²²

has completed a detailed analysis of the crystal-field splitting of the energy levels in $Ce^{3+}:CaF_2$ and tabulated the corresponding wave functions. To a first approximation, the radial parts of the ground state and the excited state are not affected by the crystal-field interactions. Under this approximation, the crystal-field and spin-orbit interactions act only on the angular and spin parts of a wave function, and those parts of the lowest $4f$ and the lowest $5d$ wave functions can be obtained from Manthey's results. For the radial parts, the free-ion radial wave functions calculated by using Fisher's multiconfigurational Hartree-Fock program²³ are used. This program also gives the total energy for the free ion in the ground and excited configurations, as well as the expectation values $\langle r \rangle_{nl}$ and $\langle r^2 \rangle_{nl}$. For other states which may be mixed into the abovementioned initial and final states, we used the free-ion wave functions.

Since the spin-orbit interaction is considerably stronger for the $4f$ states than the crystal-field interactions, the wave functions for the $4f$ states are obtained as a linear superposition of coupled $|lsjm_j\rangle$ wave functions. However, for the $5d$ states, crystal-field effects are larger than the spin-orbit effects and the Russel-Saunders states are completely mixed together. The wave functions for the $5d$ states are taken as linear combinations of product wave functions, $|lsm_l m_s\rangle = |lm_l\rangle |sm_s\rangle$. The wave functions for the lowest $5d$ state are

$$\Phi_{5d}^{(+)} = (Y_2^2 + Y_2^{-2})R_{5d}\beta/\sqrt{2}, \quad (7)$$

$$\Phi_{5d}^{(-)} = (Y_2^2 + Y_2^{-2})R_{5d}\alpha/\sqrt{2}, \quad (8)$$

where \pm corresponds to the $\pm \frac{3}{2}$ values of the crystal quantum number and the two wave functions for the lowest $5d$ state simply implies that they are still Kramer's degenerate. Writing the $|lsjm_j\rangle$ states in terms of $|lsm_l m_s\rangle$ states, we have for the lowest $4f$ state,

$$\Phi_{4f}^{(+)} = [\sqrt{5/42}(Y_3^2 + Y_3^{-2})\beta - (\sqrt{30/42}Y_3^{-3} + \sqrt{2/42}Y_3^1)\alpha]R_{4f}, \quad (9)$$

$$\Phi_{4f}^{(-)} = [\sqrt{5/42}(Y_3^2 + Y_3^{-2})\alpha - (\sqrt{30/42}Y_3^3 + \sqrt{2/42}Y_3^{-1})\beta]R_{4f}. \quad (10)$$

The \pm sign and the two wave functions again have a similar interpretation.

The one-electron levels outside of the closed Xe core for the trivalent cerium ion which lie below the conduction-band edge of CaF_2 are the $4f$, $5d$, and $6s$ levels. Since $Ce^{3+}:CaF_2$ has a single optically active electron, the states of the cerium ion may be designated by occupied one-electron levels. However, the perturbation V_{odd} of Eq. (6) cannot mix the $6s$ state with any of the $4f$ or $5d$ states in Eqs. (7)–(10). Thus the perturbation will mix only the $4f$ states with the lowest $5d$ state and only the $5d$ states with the lowest $4f$ state.

Of the seven $4f$ orbitals, only those which change sign as $z \rightarrow -z$ will be mixed into the lowest $5d$ state by V_{odd} . The corresponding $4f$ free-ion wave functions are

$$\begin{aligned} \phi_{4f}^{(1\pm)} &= (Y_3^2 + Y_3^{-2})R_{4f} \times \begin{cases} \alpha/\sqrt{2} \\ \beta/\sqrt{2} \end{cases}, \\ \phi_{4f}^{(2\pm)} &= -i(Y_3^2 - Y_3^{-2})R_{4f} \times \begin{cases} \alpha/\sqrt{2} \\ \beta/\sqrt{2} \end{cases}, \\ \phi_{4f}^{(3\pm)} &= Y_3^0 R_{4f} \times \begin{cases} \alpha \\ \beta \end{cases}. \end{aligned} \quad (11)$$

From stationary perturbation theory we then have the following form for the lowest $5d$ state in first order:

$$\Psi_{5d}^{(\pm)} = \Phi_{5d}^{(\pm)} + \sum \left[\frac{\langle \phi_{4f} | V_{\text{odd}} | \Phi_{5d}^{(\pm)} \rangle}{E(5d) - E(4f)} \right] | \phi_{4f} \rangle, \quad (12)$$

where the summation is over all of the $4f$ wave functions. Equation (12) involves a single radial integral $\langle R_{4f} | r | R_{5d} \rangle$ and angular integrals of the form $\langle Y_3^m | Y_1^0 | Y_2^m \rangle$. The radial integral has been evaluated using the Ce^{3+} radial wave functions obtained from Fischer's program²³ and has a value of 0.7398 a.u. ($= 3.91 \times 10^{-9}$ cm). The angular integrals are evaluated using the Gaunt relation²⁴ expressed in terms of the 3- j symbols. For the energy denominator in Eq. (12) we take the experimental value of $E(5d) - E(4f)$, $32\,000 \text{ cm}^{-1}$ ($= 0.146$ a.u.). Using these results, we have from Eq. (12)

$$\Psi_{5d}^{(+)} = [A_1(Y_2^2 + Y_2^{-2})R_{5d} - A_2(Y_3^2 + Y_3^{-2})R_{4f}]\alpha, \quad (13)$$

$$\Psi_{5d}^{(-)} = [A_1(Y_2^2 + Y_2^{-2})R_{5d} - A_2(Y_3^2 + Y_3^{-2})R_{4f}]\beta, \quad (14)$$

where the coefficients are $A_1 = 0.7071$ and $A_2 = 0.0511/\epsilon$.

We now calculate the mixing of the $5d$ states into the lowest $4f$ state. The free-ion wave functions are

$$\begin{aligned} \phi_{5d}^{(1\pm)} &= (Y_2^2 + Y_2^{-2})R_{5d} \times \begin{cases} \alpha/\sqrt{2} \\ \beta/\sqrt{2} \end{cases}, \\ \phi_{5d}^{(2\pm)} &= Y_2^0 R_{5d} \times \begin{cases} \alpha \\ \beta \end{cases}, \\ \phi_{5d}^{(3\pm)} &= -i(Y_2^2 - Y_2^{-2})R_{5d} \times \begin{cases} \alpha/\sqrt{2} \\ \beta/\sqrt{2} \end{cases}, \\ \phi_{5d}^{(4\pm)} &= i(Y_2^{-1} + Y_2^1)R_{5d} \times \begin{cases} \alpha/\sqrt{2} \\ \beta/\sqrt{2} \end{cases}, \\ \phi_{5d}^{(5\pm)} &= (Y_2^{-1} - Y_2^1)R_{5d} \times \begin{cases} \alpha/\sqrt{2} \\ \beta/\sqrt{2} \end{cases}. \end{aligned} \quad (15)$$

The lowest $4f$ wave functions with the first-order correction are then given by

$$\Psi_{4f}^{(\pm)} = \Phi_{4f}^{(\pm)} + \sum \left[\frac{\langle \phi_{5d} | V_{\text{odd}} | \Phi_{4f}^{(\pm)} \rangle}{E(4f) - E(5d)} \right] | \phi_{5d} \rangle, \quad (16)$$

where the summation is over all of the $5d$ wave functions. Proceeding in the same way as was done for Ψ_{5d} we obtain

$$\begin{aligned} \Psi_{4f}^{(+)} &= [B_1(Y_3^2 + Y_3^{-2})R_{4f} + B_2(Y_2^2 + Y_2^{-2})R_{5d}]\beta \\ &\quad - [(B_3 Y_3^{-3} + B_4 Y_3^1)R_{4f} + B_5 Y_2^1 R_{5d}]\alpha, \end{aligned} \quad (17)$$

$$\Psi_{4f}^{(-)} = [B_1(Y_3^2 + Y_3^{-2})R_{4f} + B_2(Y_2^2 + Y_2^{-2})R_{5d}] \alpha \\ - [(B_3Y_3^3 + B_4Y_3^{-1})R_{4f} + B_5Y_2^{-1}R_{5d}] \beta, \quad (18)$$

where the coefficients are $B_1=0.3450$, $B_2=0.0249/\epsilon$, $B_3=0.8452$, $B_4=0.2182$, and $B_5=0.0130/\epsilon$. Equations (17) and (18) give the initial states while Eqs. (13) and (14) give the final states of the zero-phonon two-photon transition in $\text{Ce}^{3+}:\text{CaF}_2$.

IV. CLOSURE APPROXIMATION

In order to evaluate the sum over intermediate states in Eq. (1) we use a closure approximation assuming a constant energy denominator. More explicitly, we take $\nu - \nu_{ig} = \Delta$ for all $|i\rangle$, and then the sum in Eq. (1) for the case of two identical photons with polarization $\hat{\mathbf{e}}$ takes the form

$$\sum_i \frac{\langle f | \hat{\mathbf{e}} \cdot \mathbf{r} | i \rangle \langle i | \hat{\mathbf{e}} \cdot \mathbf{r} | g \rangle}{\nu - \nu_{gi}} \approx \frac{\langle f | (\hat{\mathbf{e}} \cdot \mathbf{r})^2 | g \rangle}{\Delta}, \quad (19)$$

where the closure property, $\sum_i |i\rangle \langle i| = 1$, for a complete set of orthonormal eigenfunctions has been used. Equation (1) may now be rewritten as

$$\sigma = \frac{16\pi^2 \nu^2 e^4 \eta^4}{n^2 \hbar^2 c^3} \frac{|\langle f | (\hat{\mathbf{e}} \cdot \mathbf{r})^2 | g \rangle|^2}{\Delta^2} L(\nu). \quad (20)$$

There is a distinction between the use of the closure approximation made in this work and its use by Judd,⁶ Ofelt,⁷ and Axe.⁵ Judd and Ofelt treated the problem of one-photon absorption within the $4f$ configuration for rare-earth ions at noncentrosymmetric sites in crystals. The second matrix element of $(\hat{\mathbf{e}} \cdot \mathbf{r})$ in Eq. (19) is replaced by that of the odd part of the crystal-field potential for that case. The use of the closure procedure unites the dipole and the odd crystal-field operators into a single operator that acts between the $4f$ states. Axe used closure to handle the sum over the intermediate states which arises in the second-order perturbation expansions. In the present work we consider a $4f \rightarrow 5d$ two-photon transition which, like the Judd-Ofelt problem, is parity forbidden

but is induced by the odd components of the crystal field. However, in this work the form of the odd crystal field is written down explicitly and the first-order correction to the initial- and final-state wave functions are obtained using that component as a perturbation. So the closure approximation is used here not to handle the crystal field as is done in Judd-Ofelt theory, but is used more like that in Axe's treatment to deal with the sum over intermediate states in the perturbation expansion. The idea of performing closure operations piecewise in which the energy denominator is assumed to be the same for each excited configuration is central to all these calculations.

The operator $(\hat{\mathbf{e}} \cdot \mathbf{r})^2$ depends on the polarization $\hat{\mathbf{e}}$ of the incident laser beam. In order to calculate the TPA cross section using Eq. (20), we must first obtain the correct form of the operator. We assume that the laser beam is incident along the [100] direction and then consider two polarization directions: $\hat{\mathbf{e}}$ parallel to ($\theta=0^\circ$), and $\hat{\mathbf{e}}$ making an angle of 45° ($\theta=45^\circ$) with the [010] axis of the CaF_2 host. The F^- charge compensator has an equal probability of going into an interstitial site along any of the [100], [010], or [001] directions. In order to obtain the correct polarization dependence, the cross section has to be evaluated for all three orientations and then averaged. Instead of permuting the positions of the charge compensator, one may equivalently permute the directions of the polarization vector. The forms of this operator for the different permutations of the polarization direction are summarized in Table I.

The calculation of the TPA cross section using Eq. (20) for either the 0° or the 45° polarization direction is now straightforward. Matrix elements between radial wave functions of the form $\langle R_{4f} | r^2 | R_{4f} \rangle$ and $\langle R_{5d} | r^2 | R_{5d} \rangle$ were calculated from Fischer's multiconfiguration Hartree-Fock program²³ and the values obtained are $3.28 \times 10^{-17} \text{ cm}^2$ and $1.50 \times 10^{-16} \text{ cm}^2$, respectively. We have taken the local-field correction as $\eta = (n^2 + 2)/3$, where $n = 1.43$ is the CaF_2 index of refraction; $\nu = 15964 \text{ cm}^{-1}$ for excitation of the zero-phonon transition; $\Delta = 40000 \text{ cm}^{-1}$; and $L(\nu) = W^{-1} = (0.64 \text{ cm}^{-1})^{-1}$, where W is the full width at half maximum, for the zero-

TABLE I. Expression for the operator $(\hat{\mathbf{e}} \cdot \mathbf{r})^2$ for different permutations of the polarization unit vector $\hat{\mathbf{e}}$ where the unit vectors $\hat{\mathbf{x}}$, $\hat{\mathbf{y}}$, and $\hat{\mathbf{z}}$ are along the [100], [010], and [001] axes, respectively.

$\hat{\mathbf{e}}$	$(\hat{\mathbf{e}} \cdot \mathbf{r})^2 / r^2$
$\hat{\mathbf{x}}$	$1 - \sqrt{4\pi/5} Y_2^0 + \sqrt{6\pi/5} (Y_2^2 + Y_2^{-2})$
$\hat{\mathbf{y}}$	$1 - \sqrt{4\pi/5} Y_2^0 - \sqrt{6\pi/5} (Y_2^2 + Y_2^{-2})$
$\hat{\mathbf{z}}$	$1 + \sqrt{16\pi/5} Y_2^0$
$(\hat{\mathbf{x}} + \hat{\mathbf{y}}) / \sqrt{2}$	$1 - \sqrt{4\pi/5} Y_2^0 - i\sqrt{6\pi/5} (Y_2^2 - Y_2^{-2})$
$(\hat{\mathbf{y}} + \hat{\mathbf{z}}) / \sqrt{2}$	$1 + \sqrt{\pi/5} Y_2^0 - \sqrt{3\pi/10} (Y_2^2 + Y_2^{-2}) + i\sqrt{6\pi/5} (Y_2^1 + Y_2^{-1})$
$(\hat{\mathbf{z}} + \hat{\mathbf{x}}) / \sqrt{2}$	$1 + \sqrt{\pi/5} Y_2^0 - \sqrt{3\pi/10} (Y_2^2 + Y_2^{-2}) - \sqrt{6\pi/5} (Y_2^1 - Y_2^{-1})$

phonon transition.¹⁵⁻¹⁷ By substituting these values into Eq. (20), the peak two-photon absorption cross section for the zero-phonon transition is found to be

$$\begin{aligned}\sigma(0^\circ) &= (1/\epsilon^2) 2.67 \times 10^{-49} \text{ cm}^4 \text{ sec} , \\ \sigma(45^\circ) &= (1/\epsilon^2) 3.11 \times 10^{-49} \text{ cm}^4 \text{ sec} .\end{aligned}\quad (21)$$

VI. DISCUSSION

In this paper we have developed a second-order perturbation theory to calculate the two-photon absorption cross section for the lowest $4f \rightarrow 5d$ no-phonon transition in $\text{Ce}^{3+}:\text{CaF}_2$. In order to compare the results of this calculation to those obtained experimentally, we first consider the value of the polarization anisotropy defined by Eq. (3). Since it involves a ratio, and is thus independent of any overall scale factors, it is more amenable to both accurate calculation and measurement than is the absolute cross section itself. Nevertheless, the measured anisotropy is 0.5 whereas, using the cross sections from Eq. (21), the calculated anisotropy factor is only 0.076. Although the calculated value has the correct sign, it gives a much more isotropic polarization dependence to the cross section than is measured.

A much more difficult comparison to make is that for the absolute magnitudes of the TPA cross sections. The electrostatic screening of the optically active electron on the cerium ion from the electric field of the F^- charge compensator has been incorporated phenomenologically into the dielectric constant ϵ . This includes both the screening due to the ligands as well as the very strong shielding of the $4f$ electron by the filled $5s$ and $5p$ cerium orbitals²¹ and the somewhat weaker shielding of the $5d$ electron. A value of $\epsilon = 365$ would be required to bring the value of the calculated cross section into agreement with the measured value. The static dielectric constant²⁵ of CaF_2 is 7.36 which leaves about a factor of 50 to be accounted for by the Sternheimer shielding²¹ of the $4f$ electron. Given the factor-of-five uncertainty in the measured cross section and the strength of this $4f$ electron screening in other trivalent rare-earth ions,²¹ there is a reasonable agreement between the measured and calculated cross sections.

In order to account for the discrepancy between the experimental results and theoretical estimates, especially that for the polarization anisotropy, one may question the adequacy of the closure approximation. However, there are no intermediate states in near resonance with the photon frequency for which the energy denominator is small. For the $4f$ and $5d$ states in $\text{Ce}^{3+}:\text{CaF}_2$, the value of the energy denominator varies from 12400 cm^{-1} to about 37400 cm^{-1} , while for the $6s$ and conduction-band states, the value is somewhat higher. Thus the closure approximation is not too severe in this case and the inadequacy of the theory must be elsewhere.

In order to account for the integrated intensities and polarization anisotropy of the $4f \rightarrow 4f$ transition in $\text{Gd}^{3+}:\text{LaF}_3$ measured by Dagenais *et al.*,⁸ third-order perturbation terms involving spin-orbit interaction among the levels of the intermediate configurations were introduced by Judd and Pooler.¹⁰ Additional TPA measure-

ments on this system by Downer *et al.*⁹ gave results which could only be explained by invoking third and fourth-order terms¹¹ involving spin-orbit and/or crystal-field interactions among levels of the intermediate configuration. The contributions of these higher-order terms were found to be comparable to or even higher than those from the second-order terms. Thus the possibility of obtaining better agreement with experiment for the polarization anisotropy in $\text{Ce}^{3+}:\text{CaF}_2$ by using higher orders in perturbation theory cannot be ruled out. Since these higher-order terms involve levels of the same configuration, the additional energy denominators that enter into the expression for the cross section will be small for the $4f$ intermediate states in $\text{Ce}^{3+}:\text{CaF}_2$ and the corresponding contributions to the cross section may be large. As was in the case for the $4f \rightarrow 4f$ TPA transitions in $\text{Gd}^{3+}:\text{LaF}_3$, the inclusion of higher-order terms may reproduce the correct magnitude of the polarization anisotropy. However, that may increase the value of the cross section as was seen in $\text{Gd}^{3+}:\text{LaF}_3$. It is possible, however, to have destructive interference between the second-order and higher-order contributions which would reduce the magnitude of the cross section.

The polarization anisotropy of the TPA cross section is sensitive to the initial, final, and intermediate wave functions being used. In this calculation, as well as in the second-order theory of Axe⁵ and in the higher-order theories of Judd and Pooler¹⁰ and Downer and Bivas,¹¹ the participating states are all constructed from electronic configurations localized on the rare-earth ion. However, ligand-dependent effects may make significant additional contributions to the TPA cross section. There may be a small overlap between the Ce^{3+} $5d$ wave functions and the wave functions of the charge compensator and other ligands. This covalency can play a role in creating mixed-parity states. Recently Reid and Richardson¹⁴ have shown that radiation-induced ligand polarization (also called dynamic ligand polarization) may make a significant contribution to the TPA strengths. These authors considered the $4f \rightarrow 4f$ TPA transitions for the rare-earth ions and studied the contribution of dynamic ligand polarization to a third- or fourth-order TPA intensity analysis. They argued that the inclusion of this effect in the calculation leads to two different sets of intermediate states, one consisting of ligand excited states and the other includes the $4f^N-15d$ states of the rare-earth ion. Their conclusion was that a third-order process involving ligand excited states makes a contribution to the cross section which is comparable to that from the static crystal field in third order. Dynamic ligand polarization may make a significant contribution to the TPA cross section in $\text{Ce}^{3+}:\text{CaF}_2$ as well, and any future higher-order calculation should incorporate this effect.

In this work we have calculated the magnitude of the TPA cross section and its polarization anisotropy for the zero-phonon transition alone. The phonon sideband shows a frequency-dependent polarization anisotropy, which is an intrinsic feature of the $\text{Ce}^{3+}:\text{CaF}_2$ system, and may be expected in similar systems. For an allowed TPA transition²⁶ and also for the $4f \rightarrow 5d$ TPA transition in $\text{Eu}^{2+}:\text{CaF}_2$ where the ion is at a site of inversion symme-

try,²⁷ the phonon sideband has the same polarization anisotropy as would be expected of a purely electronic transition in the system under study. The Ce^{3+} ion in CaF_2 is at a site which lacks inversion symmetry and hence both even and odd vibrational modes may appear in the phonon sideband for the two-photon transition. It is this superposition of the crystal field and the vibronically induced transitions which gives the phonon sideband its frequency-dependent polarization anisotropy. A detailed quantitative analysis of this frequency dependence

presents an interesting and challenging problem for further investigation.

ACKNOWLEDGMENTS

We would like to acknowledge the financial support of the United States Department of Energy under Grant DE-FG02-84ER45056. One of us (S.K.G.) wishes to thank Professor N. Bloembergen for a helpful discussion.

*Present address: Institute for Ultrafast Spectroscopy and Lasers, Physics Department, The City College of The City University of New York, New York, NY 10031.

¹W. Kaiser and C. G. B. Garret, *Phys. Rev. Lett.* **7**, 229 (1961).

²M. Geoppert-Mayer, *Ann. Phys.* **9**, 273 (1931).

³B. Honig, J. Jortner, and A. Szoke, *J. Chem. Phys.* **46**, 2714 (1967).

⁴A. Gold and J. P. Hernandez, *Phys. Rev. A* **139**, 2002 (1965).

⁵J. D. Axe, Jr., *Phys. Rev. A* **136**, 42 (1964).

⁶B. R. Judd, *Phys. Rev.* **127**, 750 (1962).

⁷G. S. Ofelt, *J. Chem. Phys.* **37**, 511 (1962).

⁸M. Dagenais, M. Downer, R. Neumann, and N. Bloembergen *Phys. Rev. Lett.* **46**, 561 (1981).

⁹M. C. Downer, A. Bivas, and N. Bloembergen, *Opt. Commun.* **41**, 335 (1982).

¹⁰B. R. Judd and D. R. Pooler, *J. Phys. C* **15**, 591 (1982).

¹¹M. C. Downer and A. Bivas, *Phys. Rev. B* **28**, 3677 (1983).

¹²M. C. Downer, C. D. Cordero-Montalvo, and H. Crosswhite, *Phys. Rev. B* **28**, 4931 (1983).

¹³C. D. Cordero-Montalvo and N. Bloembergen, *Phys. Rev. B* **30**, 438 (1984).

¹⁴Michael F. Reid and F. S. Richardson, *Phys. Rev. B* **29**, 2830 (1984).

¹⁵S. K. Gayen and D. S. Hamilton, *Phys. Rev. B* **28**, 3706 (1983).

¹⁶S. K. Gayen, G. J. Pogatshnik, and D. S. Hamilton, *J. Lumin.* **31/32**, 260 (1984).

¹⁷S. K. Gayen, Ph.D. thesis University of Connecticut, 1984.

¹⁸M. J. Weber and R. W. Bierig, *Phys. Rev. A* **134**, 1492 (1964); J. M. Baker, E. R. Davies, and J. P. Hurrell, *Proc. R. Soc. London, Ser. A* **308**, 403 (1963), and references therein.

¹⁹M. Inoue and Y. Toyozawa, *J. Phys. Soc. Jpn.* **20**, 363 (1965).

²⁰T. R. Bader and A. Gold, *Phys. Rev.* **171**, 997 (1968).

²¹R. M. Sternheimer, M. Blume, and R. F. Peierls, *Phys. Rev.* **173**, 376 (1968).

²²W. J. Manthey, *Phys. Rev. B* **8**, 4086 (1973); W. J. Manthey, Ph.D. thesis, University of Chicago, 1972 (unpublished).

²³C. F. Fischer, *Comput. Phys. Commun.* **1**, 151 (1969); **4**, 107 (1972).

²⁴M. Weissbluth, *Atoms and Molecules* (Academic, New York, 1978), pp. 11–12.

²⁵*Handbook of Chemistry and Physics*, 52nd ed., edited by R. C. Weast (The Chemical Rubber Co., Cleveland), p. E-46.

²⁶S. A. Payne, A. B. Goldberg, and D. S. McClure, *J. Chem. Phys.* **78**, 3688 (1983).

²⁷E. Bayer and G. Schaack, *Phys. Status Solidi* **41**, 827 (1970).